Structural heterogeneity and medium-range order in Zr_xCu_{100-x} metallic glasses

Maozhi Li,[1,2] C. Z. Wang,[2,*] S. G. Hao,[2] M. J. Kramer,[2] and K. M. Ho[2]
[1]*Department of Physics, Renmin University of China, Beijing 100872, China*
[2]*Ames Laboratory, U.S. DOE, Iowa State University, Ames, Iowa 50011, USA*
(Received 1 December 2008; revised manuscript received 12 August 2009; published 2 November 2009)

Realistic three-dimensional atomistic structures of Zr_xCu_{100-x} ($x=35,50$) bulk metallic glasses are constructed using a combination of x-ray diffraction experiment and computational modeling. A cluster correlation method is developed to analyze the medium-range order in amorphous systems. We show that the glass systems consist of a stringlike backbone network formed by icosahedral clusters and a liquidlike structure filling in the remaining space. These findings are consistent with those obtained from our independent classical molecular-dynamics studies with embedded-atom method potential for ZrCu system. Such a heterogeneous structure provides a fundamental structural perspective of dynamical heterogeneity and glass formation.

DOI: 10.1103/PhysRevB.80.184201 PACS number(s): 81.05.Kf, 61.05.cp, 61.20.Gy, 61.43.Fs

I. INTRODUCTION

Describing the structure of amorphous materials such as metallic glasses has been a long-standing challenge in materials science. Despite considerable efforts in the past several decades, accurate and verifiable descriptions of the three-dimensional (3D) atomic arrangement of metallic glasses remain elusive.[1–8] The lack of detailed information on the structure of amorphous materials has limited our further understanding of dynamical properties and glass formation. For example, the concept of dynamical heterogeneity i.e., the existence of active and inactive phases in space and time in glass-forming systems has been widely accepted.[9–11] However, the question "what aspect of the structure gives rise to the dynamical heterogeneity" still remains.[9–14]

Another outstanding issue is to characterize the medium-range order (MRO) in metallic glasses. While icosahedral short-range order (SRO) was suggested as local structural unit in metallic liquids and glasses several decades ago and has been studied intensively,[15–19] recent studies have demonstrated that accurate description of amorphous structures has to consider the atomic arrangement in MRO.[4,7,8] Two structural models consisting of dense packing of atomic clusters and MRO of solute-centered clusters have been recently proposed for metallic glasses.[7,8] However, these cluster packing schemes addressed mainly the low solute concentration regime. Moreover, the issue of dynamical heterogeneity was not discussed in these models.

In this paper we address these important issues by developing a cluster correlation method to analyze the medium-range atomic arrangement in Zr_xCu_{100-x} ($x=35,50$) metallic glasses. We show that the glass structure in these systems is a heterogeneous mixture of interpenetrating icosahedral clusters forming a stringlike backbone network within a more liquidlike matrix. This finding has important ramifications on the development of glassy dynamics in the ZrCu glass-forming system.

In Sec. II, the generation of the structure models of $Zr_{50}Cu_{50}$ and $Zr_{35}Cu_{65}$ metallic glasses is described. In Sec. III, the local structure and spatial correlation of the atomic clusters are analyzed. Then we analyze the MRO and structural heterogeneity in ZrCu metallic glasses in Sec. IV. Finally, a conclusion is presented in Sec. V.

II. STRUCTURE MODELS

Binary Zr-Cu metallic systems have attracted considerable interest because of the relatively high glass-forming ability in such simple metallic systems,[20–23] which offers a good opportunity for analyzing the structural features to understand dynamical and mechanical properties in glass-forming systems.[24–29] In order to gain insights into the structural properties, we generated reliable 3D atomic structures for $Zr_{50}Cu_{50}$ and $Zr_{35}Cu_{65}$ glass alloys using a constrained reverse Monte Carlo (RMC) method[30] with the constraints being the scattering structure factor $S(q)$ from x-ray diffraction (XRD) experiment and partial pair-correlation functions (PCFs) from *ab initio* molecular-dynamics (MD) simulations.[31–33]

In our experiments, the samples of $Zr_{50}Cu_{50}$ and $Zr_{35.5}Cu_{64.5}$ metallic alloys were prepared by arc melting buttons of high-purity Zr and Cu, then rapidly cooling using a rapidly rotating Cu quench wheel. The high-energy transmission synchrotron XRD at Argonne National Laboratory was used to determine the total scattering function at room temperature.

The *ab initio* MD simulations were performed using the projector augmented-wave method within the density-functional theory as implemented in the Vienna *ab initio* simulation (VASP) package.[33] Plane-wave basis is used with an energy cutoff of 274 eV for both alloys. The simulation cell consists of 100 atoms in a cubic box with periodic boundary conditions. After being well equilibrated in the liquid states at $T=1500$ K, the systems were cooled down to 300 K at a constant cooling rate of 0.2 K/step (3 fs/step). The atomic densities of the glassy states obtained from the cooling procedure were further optimized to give zero pressure. The optimized densities are 56.66 and 62.76 atoms/nm^3 for these two glasses, respectively, which are very close to the experimental values, 57.10 and 63.70 atoms/nm^3. The structural properties of the amorphous states are then calculated by performing the statistical averages over 1000 MD steps at 300 K. For the liquid states at $T=1500$ K, atomic coordinates of 4000 MD steps were collected.

Although *ab initio* MD simulations can provide a great

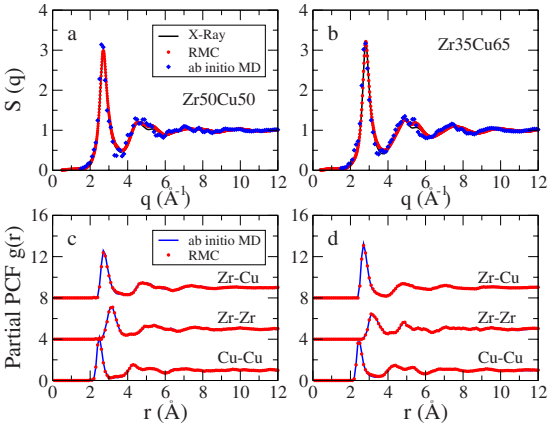

FIG. 1. (Color online) Comparison in $S(q)$ obtained from experimental XRD, *ab initio* MD, and RMC simulations for (a) $Zr_{50}Cu_{50}$ and (b) $Zr_{35}Cu_{65}$ metallic glasses. The XRD data in (b) is from a sample of $Zr_{35.5}Cu_{64.5}$ metallic glass. Comparison of *ab initio* MD and RMC derived partial PCFs for (c) $Zr_{50}Cu_{50}$ and (d) $Zr_{35}Cu_{65}$.

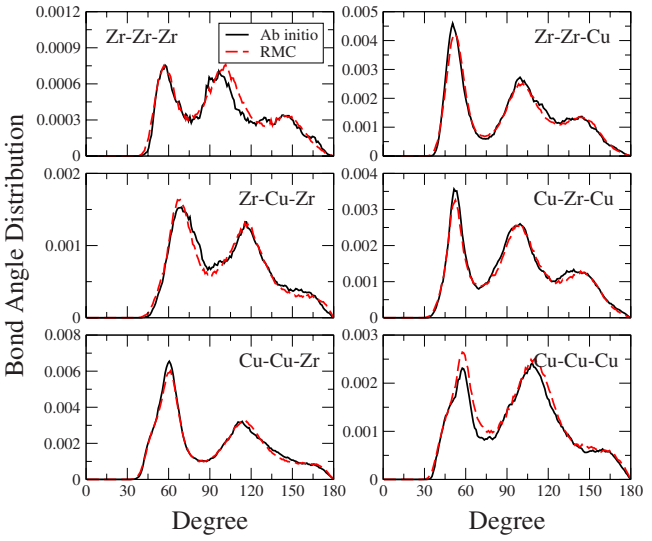

FIG. 2. (Color online) Comparison of partial bond-angle distribution functions obtained from *ab initio* MD and RMC simulations for $Zr_{50}Cu_{50}$ metallic glass.

deal of insight into the short-range structural and chemical order information, 3D atomic models with several thousand atoms or more will be more useful for studying higher-order and longer-range correlations in disordered systems. In the present study, the RMC simulations were performed to generate 3D structures with 25 000 atoms and periodic boundary conditions. Note that due to the lack of the extended x-ray-absorption fine structure (EXAFS) data from our experiments, our practical strategy in RMC modeling is to take the partial PCFs obtained from *ab initio* MD as extra constraints together with experimentally measured $S(q)$ in order to obtain a realistic glass structure.

Figure 1 shows the comparison of the structures information such as structure factor and partial PCFs obtained from the RMC simulations with those from XRD experiments and *ab initio* MD simulations for the two metallic glasses, respectively. The good agreement between the RMC and experimental $S(q)$ and between RMC and *ab initio* MD partial PCFs as shown in Fig. 1 indicate that the RMC-generated atomic configurations are reliable. Note that only the partial PCFs with r between 0 and half box size are used in the RMC fitting. Furthermore, we also compare the higher-order correlations such as partial bond-angle distribution functions from RMC models with those from *ab initio* MD simulations. Figure 2 shows a good agreement of partial bond-angle distributions between RMC modeling and *ab initio* MD simulations of $Zr_{50}Cu_{50}$ metallic glass. Note that the partial bond-angle distributions are not used as constraints in our RMC simulation.

III. LOCAL STRUCTURE AND SPATIAL CORRELATION

To examine the local structure in the RMC-generated glass models, the atomic coordinates in the models are analyzed using the Voronoi tessellation method[3,34] which divides space into close-packed polyhedra around atoms by construction of bisecting planes along the lines joining the central atom and all its neighbors. We use the Voronoi index $\langle n_3, n_4, n_5, n_6 \rangle$, where n_i denotes the number of i-edged faces of the Voronoi polyhedron, to designate the character of the atomic cluster surrounding an atom. Figures 3(a) and 3(b) show the population of the 14 most abundant polyhedra in the $Zr_{50}Cu_{50}$ and $Zr_{35}Cu_{65}$ metallic glasses, respectively. The polyhedra indices are arranged in the order of increasing coordination number (CN) of the central atoms. Most clusters with CN less than 14 are Cu centered, while those with CN larger than 14 are Zr centered due to the larger atomic size of Zr. One may note from Fig. 3 that the population of the icosahedral polyhedron $\langle 0,0,12,0 \rangle$ is relatively high in both glasses. Its fraction increases from about 3.5% to 7.4% as Cu content increases from 50% to 65%, and it is the most abundant index in $Zr_{35}Cu_{65}$. Moreover, the polyhedra of $\langle 0,0,12,0 \rangle$ are almost all Cu centered. These findings are consistent with the experimental measurements and MD simulations.[24,26]

In order to see the spatial arrangement of the $\langle 0,0,12,0 \rangle$ clusters in the glass structures, we investigated the spatial correlations between different types of Voronoi polyhedra by calculating a nearest-neighbor correlation index C_{ij} between the central atoms of polyhedra types i and j defined as follows. First let us denote m_{ij} as the number of the nearest neighbors of types i and j and P_{total} as the total number of the nearest-neighbor pairs in our structural model. Then the probability of polyhedra types i and j being the nearest neighbors can be expressed as $p_{ij}=m_{ij}/P_{\text{total}}$. On the other hand, if the distributions of indices are spatially uncorrelated, the probability of i and j being neighbors can be calculated by

$$p_{ij}^{0} = \begin{cases} \dfrac{2n_i n_j}{N(N-1)} & (i \neq j) \\ \dfrac{n_i(n_i-1)}{N(N-1)} & (i=j), \end{cases}$$

where n_i (n_j) is the number of atoms of index i (j) and N is the total number of atoms in the structural model. Finally, we

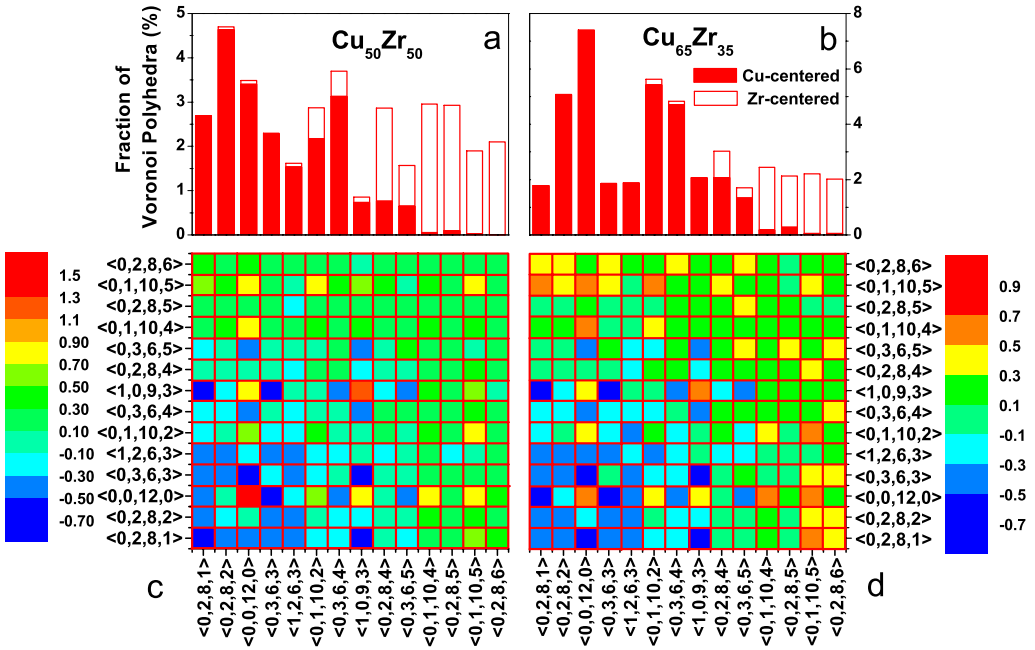

FIG. 3. (Color online) [(a) and (b)] Population and [(c) and (d)] the matrix of spatial correlation index C_{ij} of the 14 most populated Voronoi polyhedra in $Zr_{50}Cu_{50}$ and $Zr_{35}Cu_{65}$ metallic glasses. The filled and unfilled parts of each bar in (a) and (b) indicate the percentage of Cu- and Zr-centered polyhedra of each Voronoi index, respectively. The colors in (c) and (d) represent the correlation strength (see text for details).

can define the nearest-neighbor correlation index C_{ij} between polyhedra type i and type j as

$$C_{ij} = \frac{p_{ij}}{p_{ij}^{0}} - 1. \tag{1}$$

By this definition, C_{ij} is zero if the polyhedra types i and j are distributed randomly. More positive values of C_{ij} indicate stronger correlation between polyhedra types i and j (i.e., the central atoms of two polyhedra tend to be nearest neighbors), while negative values of C_{ij} indicate anticorrelation (i.e., the central atoms in two types of polyhedra avoid being nearest neighbors).

Figures 3(c) and 3(d) show the correlation matrices of C_{ij} for the 14 types of polyhedra in $Zr_{50}Cu_{50}$ and $Zr_{35}Cu_{65}$ glasses, respectively, from our RMC simulations. The correlation maps from the two glass structures exhibit a number of similar features: (i) the Cu-centered polyhedra show a preference of avoiding other Cu atoms except for the case of $\langle 0,0,12,0\rangle$ and $\langle 1,0,9,3\rangle$ which have strong tendency of clustering with themselves. (ii) Generally Zr-centered clusters have no preference of clustering with either Zr-centered or Cu-centered clusters, except in the neighborhood of $\langle 0,0,12,0\rangle$ clusters. (iii) The fact that the clustering occurs at the nearest-neighbor level indicates that the $\langle 0,0,12,0\rangle$ clusters have a strong tendency to aggregate and build interpenetrating networks with other $\langle 0,0,12,0\rangle$ clusters. (iv) Polyhedra of $\langle 0,0,12,0\rangle$ also prefer being the nearest neighbors with other polyhedra that have abundant pentagonal faces, such as $\langle 1,0,9,3\rangle$, $\langle 0,1,10,2\rangle$, $\langle 0,1,10,4\rangle$, and $\langle 0,1,10,5\rangle$, particularly when the population of $\langle 0,0,12,0\rangle$ increases as in the case with higher Cu concentrations. (v) In contrast, some abundant Voronoi polyhedra, such as $\langle 0,2,8,4\rangle$ and $\langle 0,3,6,4\rangle$, show very little preference in their nearest-neighbor indices. Such clusters can play the role of a glue to fill the 3D space in a nonpreferential fashion.

We note that strong correlation between $\langle 1,0,9,3\rangle$ is due to the fact that $\langle 1,0,9,3\rangle$ is transformed from $\langle 0,0,12,0\rangle$ when another atom is approaching to a center of threefold axis of a $\langle 0,0,12,0\rangle$ (e.g., due to fluctuation), which introduces a small triangular face. The fraction of the $\langle 1,0,9,3\rangle$ is usually very small. If such small triangular faces are removed in Voronoi analysis, most $\langle 1,0,9,3\rangle$ will be changed back to $\langle 0,0,12,0\rangle$. Therefore, $\langle 1,0,9,3\rangle$ can be classified as icosahedral cluster in our analysis. This is why $\langle 1,0,9,3\rangle$ exhibits strong correlation similar to that of $\langle 0,0,12,0\rangle$. On the other hand, a $\langle 0,1,10,2\rangle$ cluster can also be treated as an icosahedral-like cluster because it can be formed from $\langle 0,0,12,0\rangle$, too. However, they are very stable and cannot be easily changed back to $\langle 0,0,12,0\rangle$ by fluctuation.

IV. MEDIUM-RANGE ORDER AND STRUCTURAL HETEROGENEITY

Although the fraction of the icosahedral $\langle 0,0,12,0\rangle$ polyhedra is less than 8% in the glass structures, the portion of atoms belonging to this type of polyhedron is much higher, about 31% and 53% of the total number of atoms in the $Zr_{50}Cu_{50}$ and $Zr_{35}Cu_{65}$ glass alloys, respectively. The strong spatial correlation among this type of clusters as shown in Figs. 3(c) and 3(d) suggests that they would form a backbone network in the glasses.[35]

To examine the MRO of the icosahedral cluster backbone in these metallic glasses, we analyzed the connectivity of the

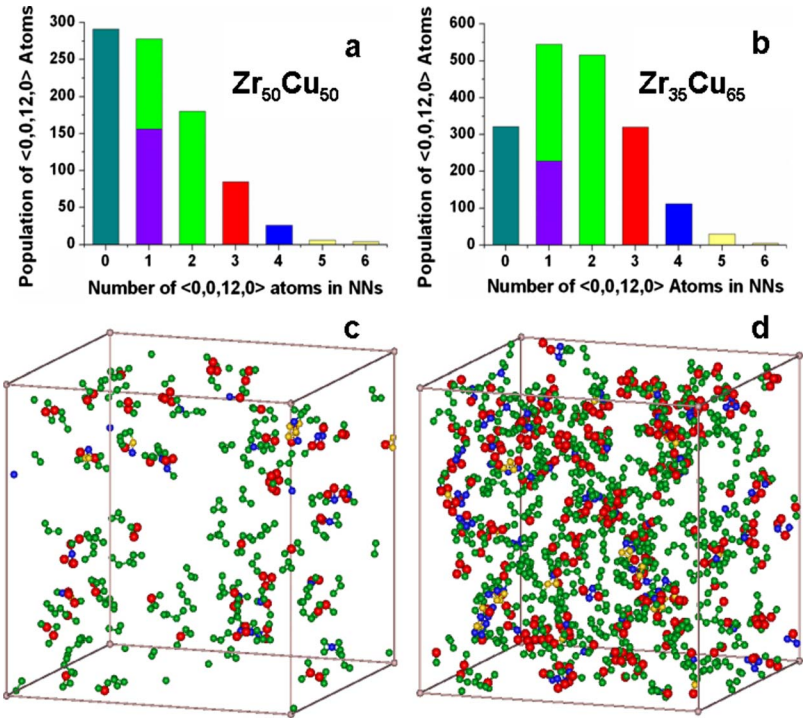

FIG. 4. (Color online) The distribution of the number of nearest-neighbor connections among the central atoms of the $\langle 0,0,12,0\rangle$ clusters (a) $Zr_{50}Cu_{50}$ and (b) $Zr_{35}Cu_{65}$. The purple and green in the second bar of (a) and (b) denote the portion of atoms belonging to dimmers or at the end of chains and branches, respectively. Spatial distribution of the central atoms of the $\langle 0,0,12,0\rangle$ clusters in (c) $Zr_{50}Cu_{50}$ and (d) $Zr_{35}Cu_{65}$. The isolated and dimerized atoms are not presented. The color schemes are the same as in (a) and (b).

network formed by the central atoms of the $\langle 0,0,12,0\rangle$ clusters.[29] The distributions of the connectivity are shown in Figs. 4(a) and 4(b) for metallic glasses of $Zr_{50}Cu_{50}$ and $Zr_{35}Cu_{65}$, respectively. Note that when a $\langle 0,0,12,0\rangle$ cluster has only one $\langle 0,0,12,0\rangle$ nearest neighbor, it can be part of a dimer or at the end of an aggregated $\langle 0,0,12,0\rangle$ chain or branch. These two situations are separated in our statistical analysis and represented using two different colors (purple for the dimers and green for the end atoms) in the column of connectivity 1 in Figs. 4(a) and 4(b). The column with connectivity of 2 is also shown in green. It can be seen that a large fraction of $\langle 0,0,12,0\rangle$ central atoms in the glasses prefers a connectivity of 2 or at the end of a chain or branch. This indicates a stringlike packing of the $\langle 0,0,12,0\rangle$ polyhedra, which can be seen in Figs. 4(c) and 4(d) where all $\langle 0,0,12,0\rangle$ central atoms, excluding monomers and dimers, are plotted. Medium-sized $\langle 0,0,12,0\rangle$ polyhedra chains ($\sim$4–5 connected clusters) can be seen to form a network throughout the glass structure. When the population of the $\langle 0,0,12,0\rangle$ polyhedra increases, more compact two-dimensional (2D) or 3D clustering of the $\langle 0,0,12,0\rangle$ polyhedra starts to emerge especially near chain junctions.

To further quantify the stringlike network formed by $\langle 0,0,12,0\rangle$ clusters, we estimate its dimensionality. For a given network, its dimension d can be obtained from the relation $N_d \sim L^d$,[36] where N_d is the total number of nodes in the network and L is a characteristic length of the network and defined as the maximum among the topologically shortest paths between all node pairs. A linear dependence of $\log(N_d)$ on $\log(L)$ is obtained as shown in Fig. 5, indicating that $d \approx 0.99 \pm 0.03$ and 1.01 ± 0.09 for $Zr_{50}Cu_{50}$ and $Zr_{35}Cu_{65}$, respectively, demonstrating the stringlike fashion of the icosahedra network. Recent studies found that icosahedral clusters slow down the dynamics in the systems.[26] The aggregation of icosahedral clusters into a stringlike backbone network may be the key factor leading to glass formation in this system by freezing out relaxation processes to prevent crystallization.

It would also be interesting to characterize the remaining structures that are not involved in the icosahedral cluster networks. As we compared the Voronoi index distribution of the glass alloys with that of the corresponding liquid alloys at 1500 K obtained from *ab initio* MD simulations, we found that they are quite different, not only on the magnitude of the distributions, but also on the types of abundant polyhedra. For example, $\langle 0,3,6,4\rangle$ is the most abundant polyhedron in

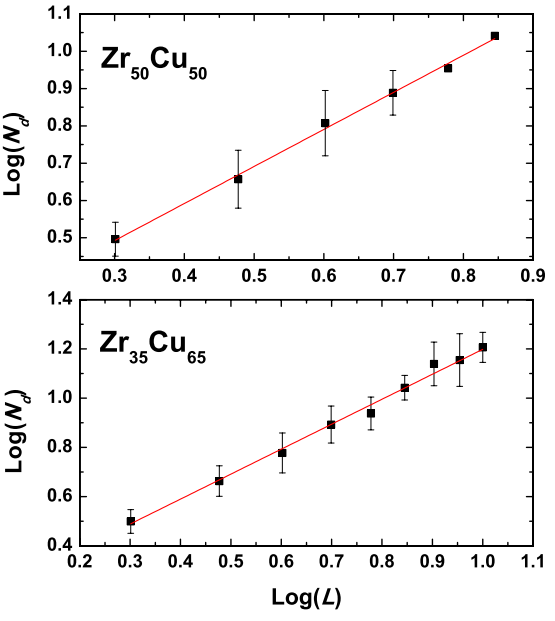

FIG. 5. (Color online) $\log(N_d)$ versus $\log(L)$ of icosahedral network in (a) $Zr_{50}Cu_{50}$ and (b) $Zr_{35}Cu_{65}$, respectively. Straight lines are the linear fit to the data.

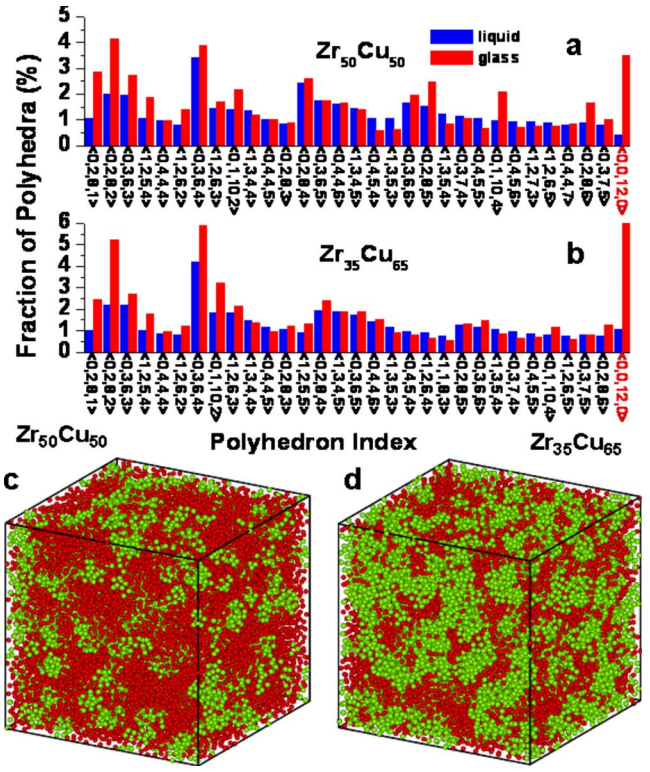

FIG. 6. (Color online) The distributions of the top 30 Voronoi polyhedra in the liquids (T=1500 K, in blue) and glasses (T=300 K, in red) of (a) $Zr_{50}Cu_{50}$ and (b) $Zr_{35}Cu_{65}$, respectively, in which the atoms belonging to the $\langle 0,0,12,0\rangle$ clusters in the liquids and glasses are excluded. The distributions are normalized by the number of atoms in the remaining parts. The atomic configurations of (c) $Zr_{50}Cu_{50}$ and (d) $Zr_{35}Cu_{65}$ metallic glasses, respectively. The green and red balls represent the atoms belonging to the $\langle 0,0,12,0\rangle$ clusters and in the remaining part of the systems, respectively. The populations of $\langle 0,0,12,0\rangle$ in liquids and glasses are also plotted for comparison.

the $Zr_{35}Cu_{65}$ liquid, while the population of $\langle 0,0,12,0\rangle$ is the highest in the glass. In liquids the population of $\langle 0,0,12,0\rangle$ is very low, 0.425% and 1.073%, in $Zr_{50}Cu_{50}$ and $Zr_{35}Cu_{65}$, respectively. However, if we exclude all the atoms belonging to the $\langle 0,0,12,0\rangle$ clusters, we found that the Voronoi distributions of the glass systems show a close resemblance to that of the corresponding liquid systems [see Figs. 6(a) and 6(b)]. This suggests that the glass structure is a heterogeneous mixture of an interpenetrating icosahedral cluster network and a liquidlike matrix.

Note that in our Voronoi analysis, the cutoff is chosen large enough (i.e., 5 Å) so that the Voronoi indices distributions are converged. We also performed the analyses using a cutoff of 4 Å [i.e., the first minimum of $g(r)$] and found that the main results and conclusions presented above do not change. Furthermore, we also performed classical MD simulation studies using the embedded-atom method (EAM) potential for ZrCu system developed in Ref. 37 and analyzed the spatial correlation of atomic clusters and the stringlike medium-range arrangement, demonstrating that the results and conclusion presented above are robust. See more details in the Appendix.

V. CONCLUSION

In summary, we have analyzed the MRO in Zr_xCu_{100-x} (x=35,50) metallic glasses. We show that Cu-centered icosahedral clusters exhibit strong spatial correlations and tend to connect with each other, forming an interpenetrating solidlike backbone with a stringlike topology. The structures filling in between the solidlike backbone are liquid like. Such a heterogeneous structure provides a fundamental structural perspective of dynamical heterogeneity in metallic glasses. The aggregation of icosahedral clusters into a stringlike backbone network may be the key process in slowing down the dynamics in these systems and leading to glass formation by freezing out relaxation processes to prevent crystallization. While the glass structures generated by our RMC modeling may be more disordered than those formed in experiments, the strong stringlike correlations between the icosahedral $\langle 0,0,12,0\rangle$ clusters and a clear picture of the structural heterogeneity have already been seen. Such MRO characters are also observed in our classical MD studies and become stronger as cooling rate decreases. We believe that the spatial correlation and structural heterogeneity will become even more evident in real metallic glasses.

Note added: Recently, we noticed that the essential structural features of the glass, i.e., "a stringlike backbone network formed by interpenetrating Cu-centered icosahedral clusters and a liquidlike structure filling in the remaining space" presented in our paper have also been mentioned in two recent published papers by Cheng *et al.*[28,29] However, our studies provide more clear evidences for these structure features.

ACKNOWLEDGMENTS

We thank J. Schmalian and R. E. Napolitano for useful discussions. Work at Ames Laboratory was supported by the (U.S.) Department of Energy, basic Energy Sciences, including a grant of computer time at the National Energy Research Supercomputing Center (NERSC) in Berkeley, under Contract No. DE-AC02-07CH11358. M.L. was also supported by NSF of China under Grant No. 10704088.

APPENDIX: CLASSICAL MD SIMULATIONS

Cooling rate used in *ab initio* MD simulations to generate glass structures from high-temperature liquids is typically about $1.0\times10^{13}\sim10^{14}$ K/s, much higher than that in experiments. It would be interesting to know to what extent the fast cooling rate influences the structures and properties of the generated metallic glasses. Specifically, since the partial PCFs obtained from our *ab initio* MD are used as constraints together with experimentally measured $S(q)$ in RMC modeling to generate larger 3D atomic structures for metallic glasses as mentioned in Sec. II, it would be desirable to know how the PCFs obtained from MD simulations are sensitive to cooling rate. Another question is whether the SRO and MRO structure features, i.e., stringlike icosahedral network and structural heterogeneity obtained from our analysis based on the RMC modeling as discussed in the text are robust or not. To investigate these two issues, we have per-

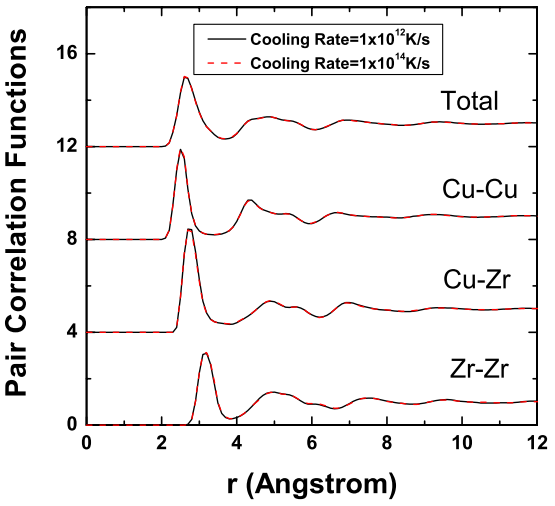

FIG. 7. (Color online) The comparison of the partial PCFs of $Zr_{35.5}Cu_{64.5}$ at $T=300$ K obtained with two cooling rates in classical MD simulations.

formed independent classical MD simulation studies with different cooling rates and analyzed the structural features of the MD-generated structure models.

In our classical MD simulations, the embedded-atom method (EAM) potential for ZrCu system developed in Ref. 37 was employed. The simulations were performed for $Zr_{35.5}Cu_{64.5}$ metallic glass. The structure model consists of 5000 atoms in the simulation cell with periodic boundary conditions. The structure was first equilibrated at $T=2000$ K, then cooled down to 300 K with cooling rate of 1.0×10^{14} and 1.0×10^{12} K/s, respectively. The cell size was adjusted to give zero pressure in *NVT* ensemble at various temperatures. The details of the generation of the structure models can be found in Ref. 38. It has been demonstrated that the structure information such as $S(q)$ in the EAM structure models shows a good agreement with experimental data.[37,38]

First we test the effect of cooling rate on the partial PCFs. Figure 7 shows the comparison of the partial PCFs of $Zr_{35.5}Cu_{64.5}$ at $T=300$ K obtained with two cooling rates in classical MD simulations. It is clear that the resulting partial PCFs are not sensitive to the cooling rate. Therefore, it should be appropriate and reliable to use partial PCFs obtained from *ab initio* MD simulations together with experimental $S(q)$ as constraints in the RMC modeling. We also found that the statistical distribution of the polyhedron types in the EAM structure models does not change much with cooling rate as shown in Figs. 8(a) and 8(b). Furthermore, the distributions are similar to that of our RMC structure model as shown in Fig. 3(b). This indicates that the structure models obtained from RMC modeling is reliable because two independent approaches generate the similar average and local structural features.

To examine the atomic cluster packing and MRO in the MD structure models, we also analyzed the spatial correlation between various clusters according to Eq. (1) for the two structures as shown in Figs. 8(c) and 8(d), respectively. It is found that the patterns of the spatial correlations between Voronoi polyhedra in the MD structure models with different cooling rates are very similar and consistent with that in RMC-generated structure models as shown in Fig. 3. This

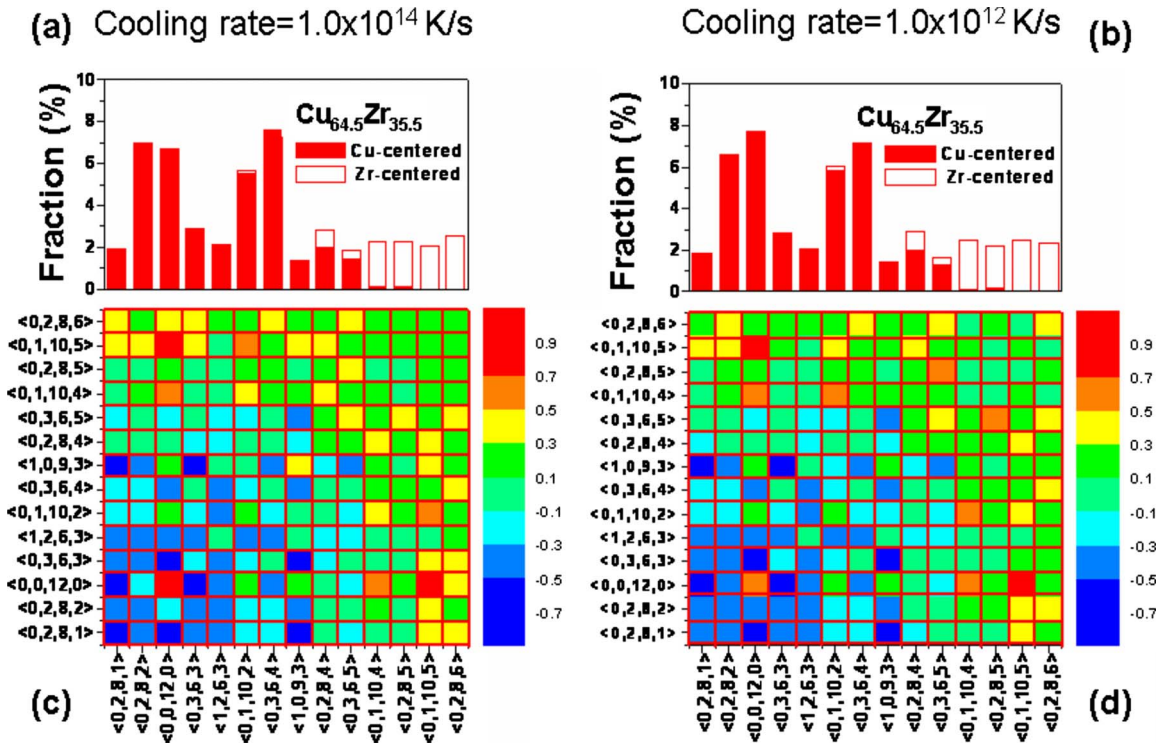

FIG. 8. (Color online) The comparison of the population and the matrix of spatial correlation index C_{ij} of the 14 Voronoi polyhedra in $Zr_{35.5}Cu_{64.5}$ metallic glasses with different cooling rates in classical MD simulations.

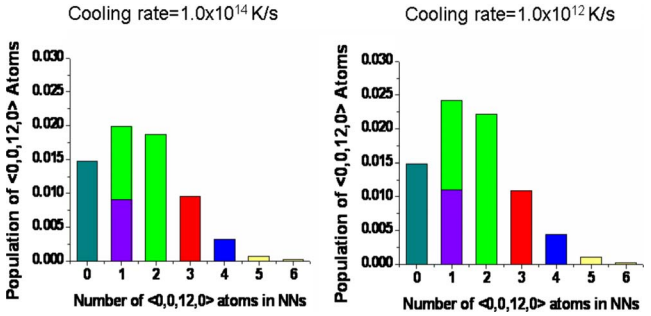

FIG. 9. (Color online) The comparison of the distribution of the number of nearest-neighbor connections among the central atoms of the $\langle 0,0,12,0\rangle$ in $Zr_{35.5}Cu_{64.5}$ metallic glasses with cooling rate of 1.0×10^{14} K/s (left panel) and 1.0×10^{12} K/s (right panel), respectively, in classical MD simulations.

indicates that the spatial correlations between clusters presented in the main text above are robust.

We also investigate the distribution of the number of nearest-neighbor connections among the central atoms of $\langle 0,0,12,0\rangle$ clusters in these two MD structure models with different cooling rates as shown in Fig. 9. It is clear that the number of $\langle 0,0,12,0\rangle$ clusters with connectivity of 2 or at the end of a chain or branch increases with decreasing the cooling rate. This indicates that the stringlike MRO will become stronger as the metallic glass structures approach to the situation of real glasses, forming a stringlike icosahedral network.

Therefore, by comparing the classical MD simulation studies, one can see that the atomic structures generated from our RMC modeling are indeed reliable, and the structural picture of stringlike icosahedral network and structural heterogeneity is robust in ZrCu metallic glasses. It is worth pointing out that although the fast cooling rate used in our AIMD and the "random" moves in RMC simulations may not capture all the details of SRO and MRO in "real-world glasses," we have already seen the strong and stringlike correlations between the icosahedral $\langle 0,0,12,0\rangle$ clusters and a clear picture for the structural heterogeneity in the metallic glasses. One can believe that the structure correlation and structural heterogeneity will become even more evident with a lower cooling rate[39] as demonstrated in our classical MD analysis.

*wangcz@ameslab.gov

[1] J. D. Bernal, Nature (London) **185**, 68 (1960).
[2] G. D. Scott, Nature (London) **188**, 908 (1960).
[3] J. L. Finney, Proc. R. Soc. London, Ser. A **319**, 479 (1970).
[4] P. H. Gaskell, Nature (London) **276**, 484 (1978).
[5] S. R. Elliott, *Physics of Amorphous Materials*, 2nd ed. (Longman, London, 1990).
[6] J. M. Dubois, P. H. Gaskell, and G. LeCaer, Proc. R. Soc. London, Ser. A **402**, 323 (1985).
[7] D. B. Miracle, Nature Mater. **3**, 697 (2004).
[8] H. W. Sheng, W. K. Luo, F. M. Alamgir, J. M. Bai, and E. Ma, Nature (London) **439**, 419 (2006).
[9] H. Sillescu, J. Non-Cryst. Solids **243**, 81 (1999).
[10] M. D. Ediger, Annu. Rev. Phys. Chem. **51**, 99 (2000).
[11] F. Ritort and P. Sollich, Adv. Phys. **52**, 219 (2003).
[12] A. Widmer-Cooper, P. Harrowell, and H. Fynewever, Phys. Rev. Lett. **93**, 135701 (2004).
[13] G. A. Appignanesi, J. A. Rodriguez Fris, and M. A. Frechero, Phys. Rev. Lett. **96**, 237803 (2006).
[14] L. Berthier and R. L. Jack, Phys. Rev. E **76**, 041509 (2007).
[15] F. C. Frank, Proc. R. Soc. London, Ser. A **215**, 43 (1952).
[16] P. J. Steinhardt, D. R. Nelson, and M. Ronchetti, Phys. Rev. B **28**, 784 (1983).
[17] H. Reichert, O. Klein, H. Dosch, M. Denk, V. Honkimaki, T. Lippmann, and G. Reiter, Nature (London) **408**, 839 (2000).
[18] T. Schenk, D. Holland-Moritz, V. Simonet, R. Bellissent, and D. M. Herlach, Phys. Rev. Lett. **89**, 075507 (2002).
[19] W. K. Luo, H. W. Sheng, F. M. Alamgir, J. M. Bai, J. H. He, and E. Ma, Phys. Rev. Lett. **92**, 145502 (2004).
[20] D. Wang, Y. Li, B. B. Sun, K. Lu, and E. Ma, Appl. Phys. Lett. **84**, 4029 (2004).
[21] M. B. Tang, D. Q. Zhao, M. X. Pan, and W. H. Wang, Chin. Phys. Lett. **21**, 901 (2004).
[22] D. H. Xu, B. Lohwongwatana, G. Duan, and W. L. Johnson, Acta Mater. **52**, 2621 (2004).
[23] P. Yu, H. Y. Bai, M. B. Tang, and W. L. Wang, J. Non-Cryst. Solids **351**, 1328 (2005).
[24] K. Park, J. Jang, M. Wakeda, Y. Shibutani, and J. Lee, Scr. Mater. **57**, 805 (2007).
[25] X. D. Wang, S. Yin, Q. P. Cao, J. Z. Jiang, H. Franz, and Z. H. Jin, Appl. Phys. Lett. **92**, 011902 (2008).
[26] Y. Q. Cheng, H. W. Sheng, and E. Ma, Phys. Rev. B **78**, 014207 (2008).
[27] Y. Q. Cheng and E. Ma, Appl. Phys. Lett. **93**, 051910 (2008).
[28] Y. Q. Cheng, A. J. Cao, and E. Ma, Acta Mater. **57**, 3253 (2009).
[29] Y. Q. Cheng, E. Ma, and H. W. Sheng, Phys. Rev. Lett. **102**, 245501 (2009).
[30] R. L. McGreevy, J. Phys.: Condens. Matter **13**, R877 (2001).
[31] M. C. Payne *et al.*, Rev. Mod. Phys. **64**, 1045 (1992).
[32] G. Kresse and J. Hafner, Phys. Rev. B **47**, 558 (1993).
[33] G. Kresse and J. Furthmuller, Comput. Mater. Sci. **6**, 15 (1996).
[34] V. A. Borodin, Philos. Mag. A **79**, 1887 (1999).
[35] Y. Shi and M. L. Falk, Scr. Mater. **54**, 381 (2006).
[36] J. Feder, *Fractals* (Plenum, New York, 1988).
[37] M. I. Mendelev, D. J. Sordelet, and M. J. Kramer, J. Appl. Phys. **102**, 043501 (2007).
[38] M. I. Mendelev, D. K. Rehbein, R. T. Ott, M. J. Kramer, and D. J. Sordelet, J. Appl. Phys. **102**, 093518 (2007).
[39] D. Ma, A. D. Stoica, and X. L. Wang, Nature Mater. **8**, 30 (2009).